Sensors and Materials, Vol. 35, No. 5 (2023) 1715–1730
MYU Tokyo

S & M 3282

Using ANSYS Workbench as a Tool to Simulate and Analyze the Effects of Different Loads on Single-layer Reticulated Aluminum Domes

Budhi Bakhtiar,[1,2] Shen-Chih Yang,[3] Chao-Ming Hsu,[3*]
Kuo-Kuang Fan,[1] and Cheng-Fu Yang[4,5**]

[1]Graduate School of Design, National Yunlin University of Science & Technology, Douliou, Yunlin 64002, Taiwan
[2]Electro Engineering Department, Padang State Polytechnics, West-Sumetera, Indonesia
[3]Department of Mechanical Engineering, National Kaohsiung University of Science and Technology, Kaohsiung 807, Taiwan
[4]Department of Chemical and Materials Engineering, National University of Kaohsiung, Kaohsiung 811, Taiwan
[5]Department of Aeronautical Engineering, Chaoyang University of Technology, Taichung 413, Taiwan

(Received January 7, 2023; accepted April 26, 2023)

Keywords: analysis and design, single-layer, reticulated aluminum dome, ANSYS Workbench

The unique structure of single-layer reticulated aluminum domes allows for an even distribution of tension throughout their whole structures to support their own weights. Two different methods are used to determine the effects of different loads on the single-layer reticulated aluminum domes. The first method uses sensors attached to the dome and the second method uses software simulation; the second method was used in this study. To obtain a better understanding of the maximum and minimum principal stresses, we conducted the parametric analyses of domes through simulations using the finite element method (FEM) software ANSYS Workbench to improve our understanding of the maximum and minimum principal stresses, stress distributions, and maximum deformations of designed single-layer reticulated domes under four different load conditions (static, average live, uneven live, and wind loads). Mixed-type reticulated domes with the hybrid structure of the Kiewitt and joint-square types were adopted in this study. In finite element method (FEM) analyses, the designed domes were subjected to six different load conditions to simulate their three principal stresses and maximum deformations. The purpose was to determine whether the 6061-T6 aluminum alloy material used in the domes would fail by reaching its yield strength. The analysis results showed that when the six different load conditions were applied to two types of dome, their maximum stresses were much smaller than the maximum stress of the material used, and the two designed domes met safety specification standards.

1. Introduction

A fixed dome can effectively isolate the contact between the inner floating roof and the outside, and thus it can ensure that the inner floating roof operates under controllable

*Corresponding author: e-mail: jammy@nkust.edu.tw
**Corresponding author: e-mail: cfyang@nuk.edu.tw
https://doi.org/10.18494/SAM4321

ISSN 0914-4935
https://myukk.org/

environmental conditions, thereby considerably improving its service life. Since the problem of corrosion caused by foreign objects is largely eliminated, the technical requirements and costs required in the manufacture of the combination of the inner floating roof and the fixed dome are also considerably reduced. Many research studies have been performed to determine the effects of different loads on the static and dynamic stabilities of a designed dome. In 1997, Uematsu *et al.* published the results of a fundamental study on the wind loads and wind-induced dynamic properties of a long-span dome with the structure of a rigidly connected single-layer lattice.(1) In 1999, Wang and Shen used a Lagrangian formulation to perform three-dimensional beam element geometry nonlinear analyses, which included the joints of large rotations and displacements under strong wind load and earthquake action.(2) In 2001, Uematsu *et al.* published some basic research results on wind-induced dynamic characteristics and the synthetic load estimation of a single-layer reticulated dome blown by wind for a prolonged period.(3) López *et al.* used the numerical analysis method to quickly estimate the buckling loads of semi-rigidly connected single-layer lattice domes under symmetrical load conditions.(4)

In 2012, Fan *et al.* took the Kiewitt-6 and Kiewitt-8 single-layer reticulated shell structures as examples and used the ANSYS Workbench as the simulation FEM software to quantitatively determine the effect of the initial curvature of the component on the ideal and node deviation structures.(5) The method they adopted can be used to effectively judge the component buckling of reticulated shell structures and proved that the component buckling and its propagation can directly affect the stability of the structure.(6) On the basis of parametric study results and the comparison with other traditional stability analysis methods, Liu *et al.* found that the random defect modal superposition method provides high accuracy at considerably low computational cost.(7) In 2017, Jihong and Nian developed a new numerical analysis method for the study of complex mechanical behavior, including the large deformation, material nonlinearity, and fracture of large or very large components.(8) Nie *et al.* used increment dynamic analysis to determine the effect of seismic load on a single-layer reticulated dome.(9) Dimopoulos and Gantes used the numerical methods GMNIA and MNA/LBA to design cylindrical steel shells with a reinforced or unreinforced rectangular cutout.(10) Sharbaf *et al.* used Karamba3D analysis to define the masonry dome behaviors on the basis of the support condition's effect of a designed dome on thickness and curve parameters.(11) Opatowicz *et al.* used geometric nonlinear analysis to assess the effect of wind load on the load capacity of a single-layer bar dome.(12)

In the past, there were two different methods used to determine the effects of different loads on single-layer reticulated aluminum domes; the first uses sensors attached to the dome. For example, Nie and Liu selected three-dimensional acceleration sensors attached to eight groups of measuring points to determine the dynamic response of acceleration.(13) Zhao *et al.* used displacement sensors to study the mechanical properties of a single-layer aluminum-alloy combined lattice shell structure.(14) These research studies described in Refs. 9–11 suggest that using a simulation method to design a dome and find its stability under different loads is highly efficient and valid. Because when a simulation method is used, researchers do not need to spend a lot of money for the construction of a real dome. However, most research studies show that only a single variable was used as the simulation parameter on a designed dome. In an actual situation, there will be many different loads simultaneously acting on a dome, and only a few

research studies focused on the effects of different loads on the stability of a designed dome. The primary focus or innovative aspect of this study is the analysis of how various loads affect stress and deformation variations in the designed dome structure. With the rapid development of computer technology, it is feasible to solve more complex nonlinear problems by the simulation method. The method of using numerical analysis to simulate the stress state of a structure and then to predict the stress and deformation of a structure is also widely used. Compared with other dome types, single-layer reticulated aluminum domes have many competitive advantages such as low weight, sturdiness, high durability, low cost, easy to assemble and disassemble, and easy to maintain. Therefore, in this study, we used the FEM analysis software ANSYS Workbench to simulate the changes in single-layer reticulated aluminum domes using two different connection methods, welding and sliding bases.

In this research, six different load conditions (static load, static load + average live load, static load + uneven live load, static load + wind load, static load + average live load + wind load, and static load + uneven live load + wind load) were used as simulation parameters. We utilized various load conditions, including two or three distinct loads, to assess the stability of the single-layer reticulated aluminum domes we designed. By analyzing factors such as the maximum and minimum principal stresses and total deformation, we were able to confirm that the domes can withstand an internal stress (static load) as well as external stresses, such as uneven live, average live, and wind loads. Our main consideration is the structure failure causing (a) stresses attributable to external forces exceeding the material yield stress and (b) permanent deformations caused by external force. We will show that for two domes under the six different loads, their maximum stresses are much smaller than the maximum stress of the material used (6061-T6 aluminum alloy), and the deformation will not be permanent.

2. Simulation Process and Parameters for Simulation

To fabricate high-security single-layer reticulated aluminum domes and maintain their functions under various climatic conditions and other natural or man-made pressures, API Standard 650: Appendix G had established relevant standard design loads. To ensure their safety and stability, the designed single-layer reticulated aluminum domes have been subjected to structural analysis and simulation designs in accordance with the applicable standards. API Standard 650: Appendix G stipulates that the maximum radius of curvature (R) of a single-layer mesh aluminum dome cannot be greater than 1.2 times the diameter (D) of the barrel tank, and the minimum R cannot be less than 0.7 D. The R/D ratio will affect the shape and bearing capacity of the dome. For the designed domes, the span was 47.65 m, the ratio of the radius of curvature of the domes to the diameter of the barrel tank was set to 1, as shown in Fig. 1(a), and the height was 6.38 m, as shown in Fig. 1(b). As shown in Fig. 1(a), the connection methods of the domes and barrel tank are also worth discussing. For that, two types of connection method, welding base (abbreviated as dome 1) and sliding base (dome 2), were designed. Because six different load conditions were used here, the different connection methods were used to compare the loading effects on the domes' three principal stresses and the maximum deformations under different load conditions.

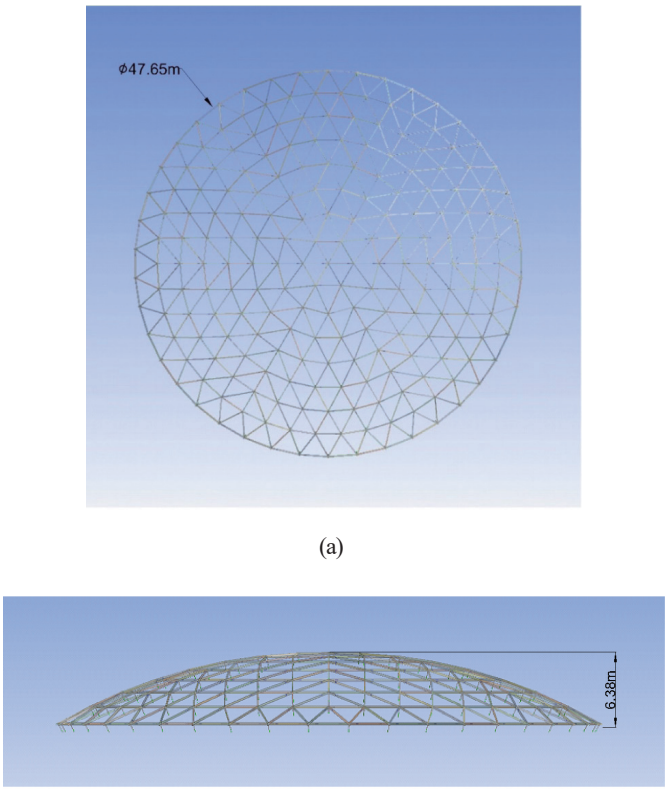

(a)

(b)

Fig. 1. (Color online) Schematic of the model of the designed dome. (a) Top and (b) side views.

At present, dome designers have many experiences in using Kiewitt-type reticulated domes for installing and constructing storage tanks. Therefore, the Kiewitt-type reticulated domes were used as the designed structure for processing simulations. However, owing to the support of the ring beam at the outermost end of the reticulated shell, the outermost ring of the Kiewitt structure experiences a non-uniform stress. If the supports are distributed in this way, it will be unfavorable for the lower tank body. Several circles of square grids make the stress distribution of the bearing on the ring beam more uniform, which can improve the uneven stress. To sum up these descriptions, according to the structural characteristics of the large-scale storage tank, the mixed-type reticulated domes with the hybrid structure of the Kiewitt and joint-square types were designed. As for the section of the rods, because they were different from the reticulated domes, the skins of the reticulated domes of the storage tanks were in direct contact with the rods. The rods needed to bear the bending moment, so they should not be a round tube, and the use of I-beam members was preferred. Correspondingly, the connections between the I-beam members should be in the form of plate-type nodes, not socket-type nodes. For that, the cross sections of the I-structural beams in the single-layer reticulated aluminum domes were adjusted for different positions. Table 1 shows the dimensions of various I-structural beams used in the Kiewitt and lamella types, along with the tension ring and shoe beam.

Table 1
Sizes of different I-structural beams. h: height, b: flange width, A_g: cross-sectional area of beam.

Region	h (mm)	b (mm)	flange t (mm)	web t (mm)	A_g (cm^2)
Kiewitt	200	100	4.5	3.5	15.685
Lamella	200	120	7.0	5.0	26.100
Tension ring	200	150	9.0	7.0	39.740
Shoe beam	200	150	9.0	7.0	39.740

The designed single-layer reticulated aluminum domes used two connection methods; therefore, there were different boundary conditions. First, a fixed support was set at the end of the support beams in the outermost ring, which restricted all its degrees of freedom. This setting was for simulating the method of welding the domes to the tank walls. Then, the sliding supports at the end point of the outermost support beams were converted to the cylindrical coordinate method, and all the degrees of freedom were restricted. This means that only the radial translation was free; this condition was used to simulate the installation of a dome on the sliding tank. In terms of loads, in addition to the static load representing its own weight, there were also live and wind loads that needed to be applied to the domes. The live load can be divided into the average and uneven live loads. The allowable load W_a includes the static and live loads (kPa), and it is defined as

$$W_a = \frac{108.1\times10^6\sqrt{I_x A_g}}{(SF)LR^2}, \tag{1}$$

where I_x is the moment of inertia of the support member on the principal plane of the domes' surface (cm^3), A_g is the cross-sectional area of the beams (cm^2), R is the radius of curvature of the domes (cm), L is the average length of the beams (cm), and SF is the safety factor and it is equal to 1.65.

The static load is the weight of an object, that is, the total weight of all components in the object, including those of beams, sheets, battens, gussets, and fasteners. The total weight or total static load of the designed single-layer reticulated aluminum domes and their accessories is approximately 270000 N. The live load (also called the dynamic load) is mainly the load caused by external factors, which can represent the load imposed by a foreign object placed on the single-layer reticulated aluminum domes. The live load can be divided into the average and uneven live loads, as shown in Figs. 2 and 3. First, the designed dome model was imported into ANSYS Workbench. Next, the material parameters for different I-structural beams were set, and then the dome model was meshed. After the boundary conditions were set, ANSYS Workbench was used to simulate actual situations. According to the specifications outlined in API Standard 650: Appendix G, an average live load of 1 kPa was applied to all domes, while a minimum uneven live load of 0.5 kPa was applied to half of the designed domes. From the API Standard 650, the minimum wind load was the load caused by the static wind pressure of 1.48 kPa, which was imposed by the wind of 190 km/h. Under this condition, the wind load was obtained as

$$\text{Wind pressure} = 1.48 \times (155/190)^2 = 0.982 \text{ kPa}. \tag{2}$$

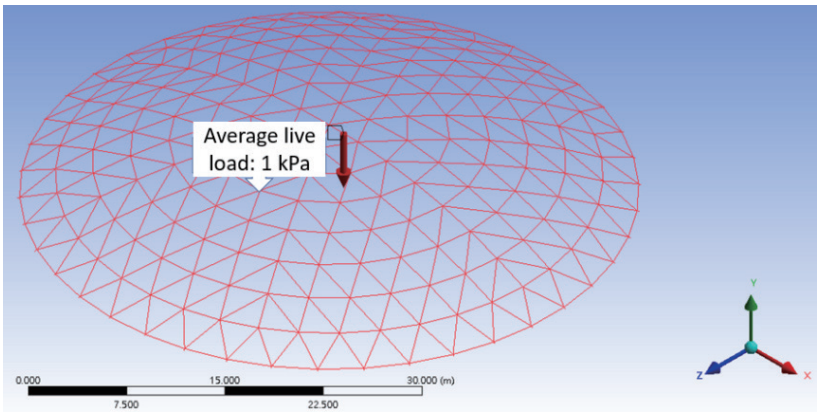

Fig. 2. (Color online) Schematic of average live load.

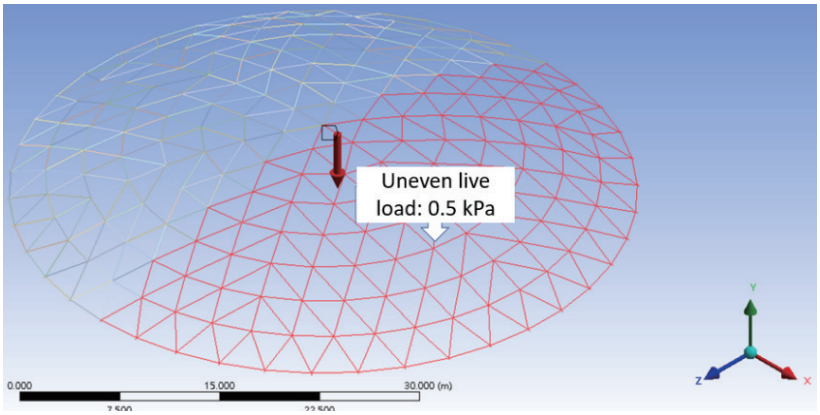

Fig. 3. (Color online) Schematic of uneven live load.

The wind load was determined to be the pressure coefficient multiplied by the wind pressure.

$$\text{Windward (1/4)} = -0.9 \times 0.982 = -0.884 \text{ kPa} \tag{3}$$

$$\text{Middle ward (1/2)} = -0.7 \times 0.982 = -0.688 \text{ kPa} \tag{4}$$

$$\text{Leeward (1/4)} = -0.5 \times 0.982 = -0.491 \text{ kPa} \tag{5}$$

In this study, 6061-T6 aluminum alloy was used as the material of the I-beams in the single-layer reticulated aluminum domes. The 6061-T6 aluminum alloy has high strength and is lighter than ordinary steels, and it is very suitable for constructing the structure of the domes, which require high strength and light weight. Since the change in ambient temperature was not discussed in this study, only the material property parameters at room temperature were used, and the values are shown in Table 2. The single-layer reticulated aluminum domes were subjected to the six load conditions, which are shown in Table 3, for simulations to test whether the domes met the safety specifications.

Table 2
Material properties of 6061-T6 aluminum alloy.

Material property	Value
Ultimate tensile stress	310.0 MPa
Yield stress	280.0 MPa
Young's modulus	71000 MPa
Unit weight	27173.7 N/m^3
Poisson's ratio	0.33

Table 3
Load conditions for the designed dome.

Condition 1	Static load
Condition 2	Static load + average live load
Condition 3	Static load + uneven live load
Condition 4	Static load + wind load
Condition 5	Static load + average live load + wind load
Condition 6	Static load + uneven live load+ wind load

3. Simulation Results and Discussion

Large-scale reticulated storage tanks mostly use single-layer spherical reticulated domes, which have two main structures: spatial triangular reticulated and spatial quadrilateral meshed reticulated domes. The former includes structural forms such as the rib ring, Kiewitt, joint square, and geodesic types, and the latter is called the Hamman grid reticulated dome. In terms of strength, stiffness, and stability, the spatial triangular reticulated dome is better than the spatial quadrilateral meshed reticulated dome, because the latter is extremely sensitive to non-uniform asymmetric loads.[15] Therefore, we used the spatial triangular reticulated dome as our mainly designed structure. According to the elasticity theory, an infinitesimal volume of material at any point or inside a solid can be rotated such that only principal stresses are still kept and all shear stresses are zero. The remaining three principal stresses are called principal stresses.[16] The maximum principal stress (σ_1), the middle principal stress (σ_2), and the minimum principal stress (σ_3) are the main stresses to be discussed, and the relationships between the three principal stresses are $\sigma_1 > \sigma_2 > \sigma_3$. The three parameters are combined with the allowable stress design (ASD) method to judge whether the material of the domes is deformed or damaged.

The results that should be simulated and analyzed are the maximum and minimum principal stresses and the total deformation of the designed single-layer reticulated aluminum domes. Once these values were determined, the maximum and minimum principal stresses with larger magnitudes were selected to work in conjunction with the ASD method, and multiplied by the *SF* of 1.65. Then, the obtained values were used to judge whether the designed domes have met the standard safety requirements. The allowable stress σ_a is the basic parameter for considering whether the dome material has deformed in the design process. The σ_a of the designed domes can be obtained by multiplying the yield stress σ_y of the dome material with the *SF* of 1.65.

$$\sigma_a = \sigma_y / SF \text{ and } \sigma_a = 280 \text{ MPa} / 1.65 = 169.7 \text{ MPa} \quad (6)$$

Therefore, as long as the maximum values of the principal stresses σ_1 and σ_3 (the maximum values of the principal stress σ_{max}) of the designed domes are greater than 169.7 MPa, the designed domes applied with different loads will exceed the limit of the yield stress of the material used and will not meet the safety specifications. In contrast, if the maximum value of the principal stress σ_{max} is less than 169.7 MPa, the designed domes can withstand the different loads applied and thus meet the safety specifications. The analysis and simulation results of the six different loads on the two designed domes are shown and discussed below.

3.1 Static load

A dome experiences an initial stress due to the static load caused by its own weight; therefore, considering this load in the analysis of the initial stress is crucial. Under this condition, only the static load was applied to the domes, and the analysis results of dome 1 are shown in Fig. 4.

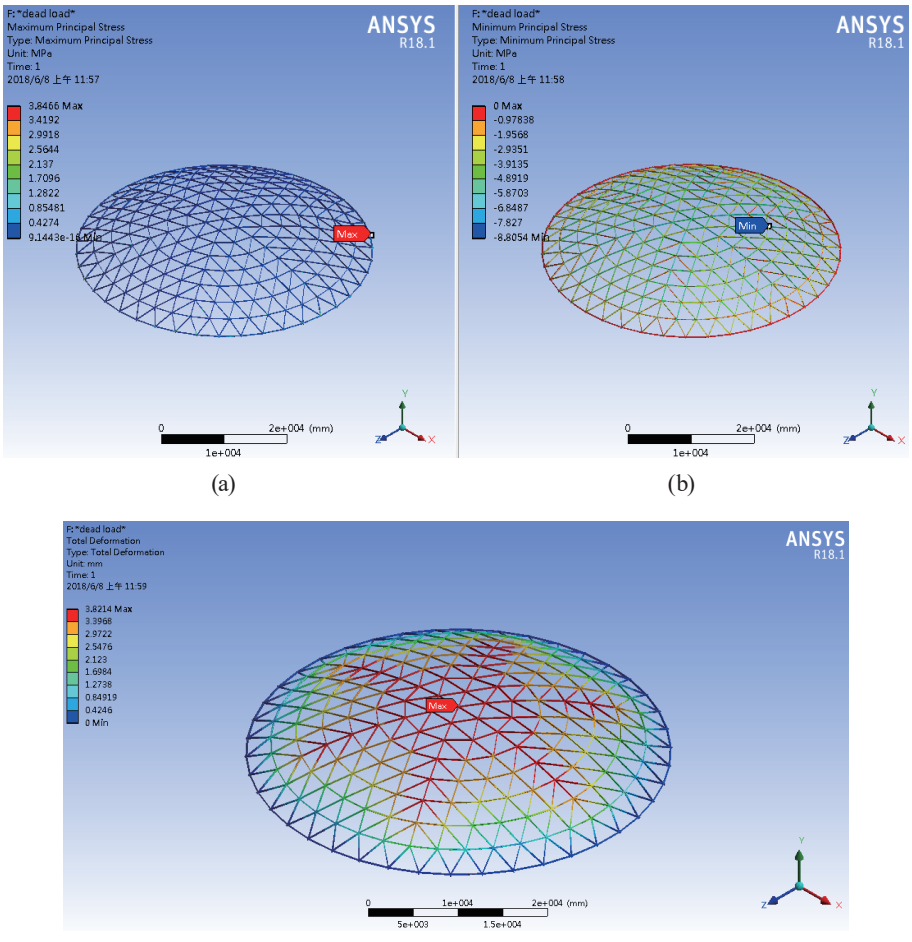

Fig. 4. (Color online) Dome 1 with static load. (a) Maximum and (b) minimum principal stresses, and (c) maximum deformation.

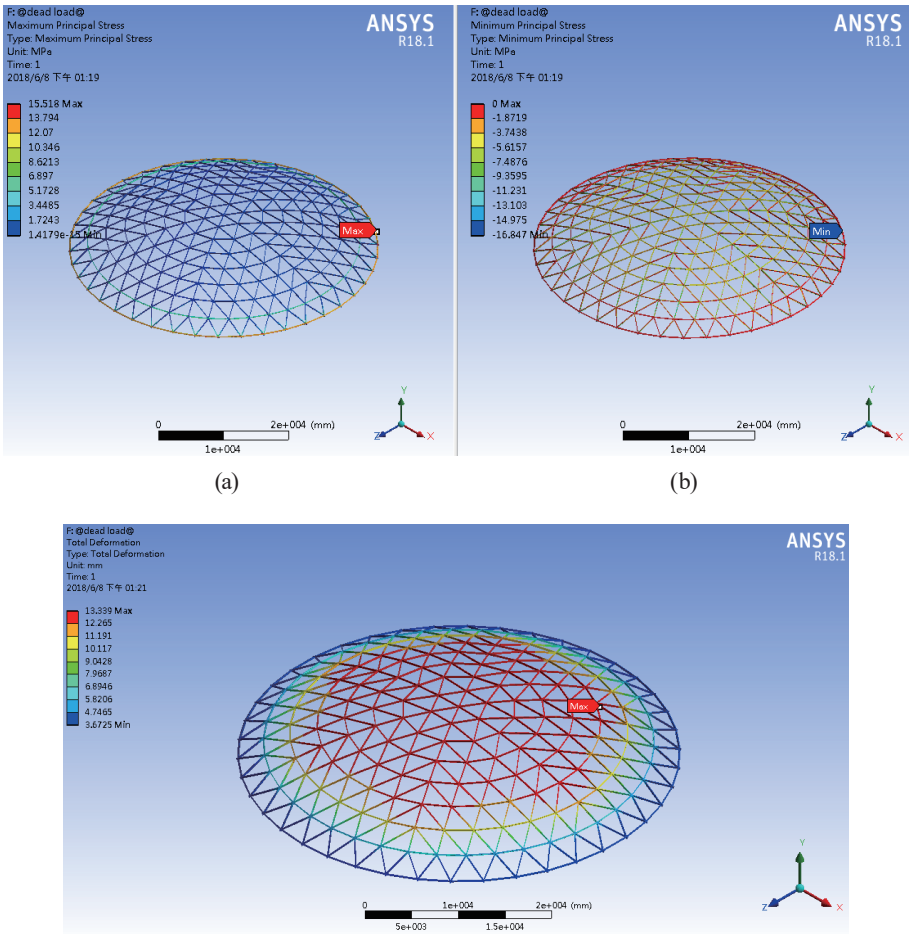

Fig. 5. (Color online) Dome 2 with static load. (a) Maximum and (b) minimum principal stresses, and (c) maximum deformation.

Figures 4(a)–4(c) show that σ_1 was 3.85 MPa, σ_3 was −8.81 MPa, and the maximum deformation was 3.82 mm, respectively. The analysis results of dome 2 indicated in Figs. 5(a)–5(c) show that σ_1 was 15.52 MPa, σ_3 was −16.85 MPa, and the maximum deformation was 13.34 mm, respectively. These results comply with safety regulations. Under the static load condition, the σ_1, σ_3, and maximum deformation values of the designed domes 1 and 2 are small, and those of dome 2 are larger than those of dome 1.

3.2 Static load + average live load

The static and average live loads were simultaneously applied to the designed domes, and the simulation results of dome 1 were subsequently analyzed (not shown here). The analysis results of dome 1 showed that σ_1 was 27.27 MPa, σ_3 was −74.29 MPa, and the maximum deformation was 32.45 mm. The analysis results of dome 2 are shown in Fig. 6. Figures 6(a)– 6(c) show that σ_1 was 124.87 MPa, σ_3 was −135.38 MPa, and the maximum deformation was 111.88 mm,

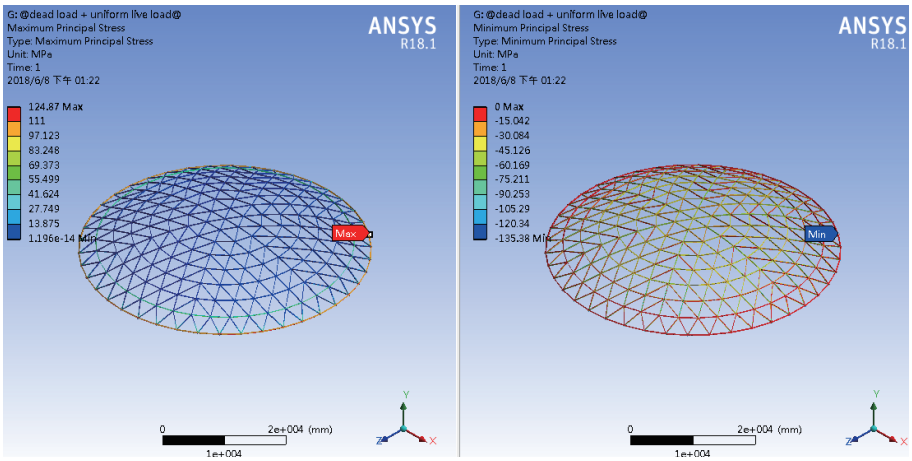

Fig. 6. (Color online) Dome 2 with static load + average live load. (a) Maximum and (b) minimum principal stresses, and (c) maximum deformation.

respectively. These results are in compliance with safety regulations. Under the condition of static load + average live load, the σ_1, σ_3, and maximum deformation values of the designed domes 1 and 2 were much larger than those when only the static load was applied. These results suggest that the average live load is an important factor that affects the safety of the designed dome. When the different loads were applied to the designed domes, the deformation of the domes stopped in the same direction after minimal vibration. Because a live load is uniformly distributed and eventually factored into the calculation of gravity loads, it can act on a concentrated area to form a point load. Therefore, if the static and average live loads are applied simultaneously, the σ_1, σ_3, and maximum deformation values will become larger than those under other conditions. However, the σ_1, σ_3, and maximum deformation values of dome 2 were much larger than those of dome 1, suggesting that the structure of dome 1 is stabler and safer than that of dome 2.

3.3 Static load + uneven live load

In this simulation scenario, both the static and uneven live loads were applied simultaneously, and the resulting analysis of dome 1 was examined (not shown here). The analysis results of dome 1 show that σ_1 was 54.21 MPa, σ_3 was −76.28 MPa, and the maximum deformation was 29.62 mm. The analysis results of dome 2 are shown in Fig. 7. Figure 7(a)–7(c) show that σ_1 was 73.22 MPa, σ_3 was −78.43 MPa, and the maximum deformation was 59.21 mm, respectively. The simulation results indicated that when both the static and uneven live loads were applied, the σ_1, σ_3, and maximum deformation values of both the designed domes 1 and 2 were greater than those observed when only the static load was applied. This was attributed to the impact of the uneven live load. These simulation results of the σ_1, σ_3, and maximum deformation of the designed domes 1 and 2 were also in compliance with safety regulations. These results suggest that even if the static and uneven live loads are simultaneously applied to the two different domes, their σ_1, σ_3, and maximum deformation values will not be significantly different.

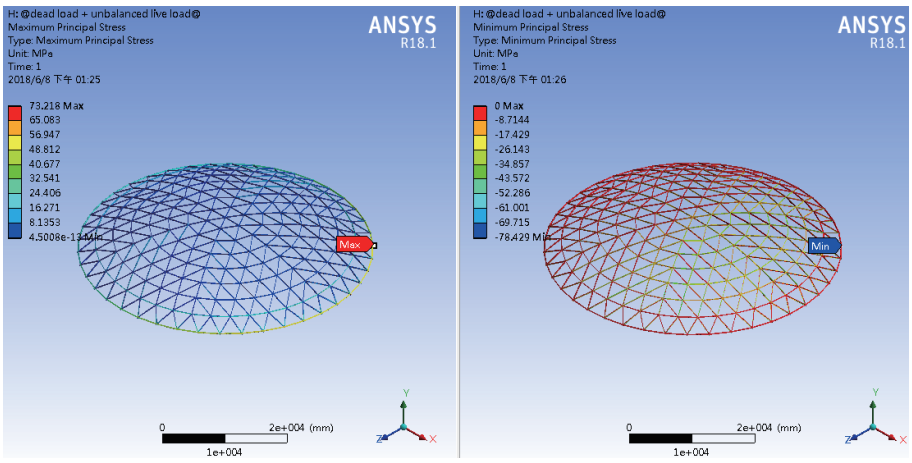

Fig. 7. (Color online) Dome 2 with static load + uneven live load. (a) Maximum and (b) minimum principal stresses, and (c) maximum deformation.

3.4 Static load + wind load

Flowing winds generate fluctuating wind loads or wind pressures on domes, and they are important factors that affect the stability of a constructed long-span dome. Under this simulation condition, the static and wind loads were applied simultaneously, and the analysis results of dome 1 (Fig. 8) show that σ_1 was 47.56 MPa, σ_3 was −20.74 MPa, and the maximum deformation was 20.37 mm. The analysis results of dome 2 (not shown here) show that σ_1 was 75.93 MPa, σ_3 was −70.27 MPa, and the maximum deformation was 61.67 mm. The simulation results of the σ_1, σ_3, and maximum deformation of the designed domes 1 and 2 are also in compliance with safety regulations, and even the σ_1, σ_3, and maximum deformation values of dome 2 are much larger than those of dome 1. These results suggest again that the structure of dome 1 is stabler and safer than that of dome 2.

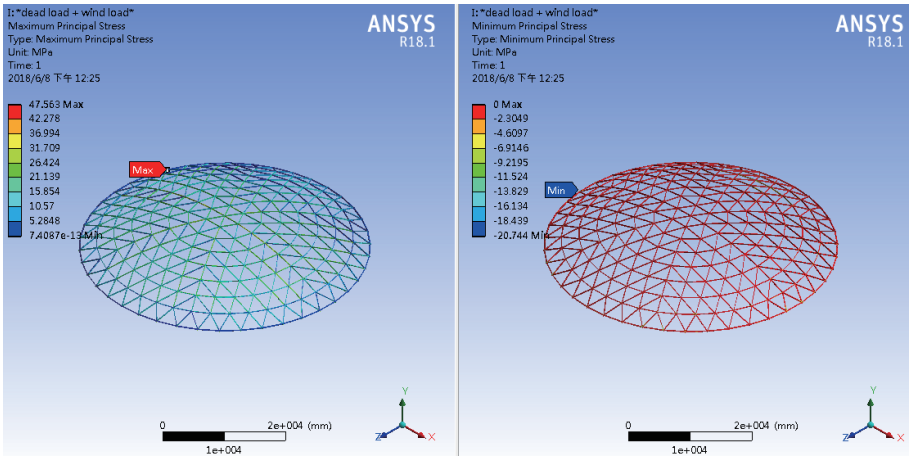

(a) (b)

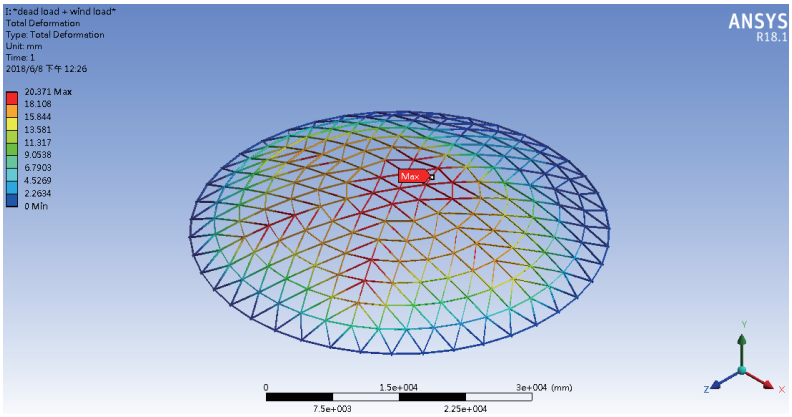

(c)

Fig. 8. (Color online) Dome 1 with static load + uneven live load. (a) Maximum and (b) minimum principal stresses, and (c) maximum deformation.

3.5 Static load + average live load + wind load

Under this simulation condition, the static, average live, and wind loads were applied simultaneously, and the analysis results of dome 1 (Fig. 9) show that σ_1 was 35.39 MPa, σ_3 was −58.77 MPa, and the maximum deformation was 60.11 mm. The analysis results of dome 2 (not shown here) show that σ_1 was 72.40 MPa, σ_3 was −77.83 MPa, and the maximum deformation was 60.11 mm. Under the simulation scenario where the static, average live, and wind loads were applied simultaneously, the σ_1, σ_3, and maximum deformation of dome 1 showed negligible changes in comparison with the case where only the static and average live loads were applied. However, in the case of dome 2, the σ_1, σ_3, and maximum deformation values were significantly decreased when the static, average live, and wind loads were applied simultaneously, compared with the case where only the static and average live loads were applied. One possible explanation for this outcome is that the direction of the force generated by the wind differs from that when

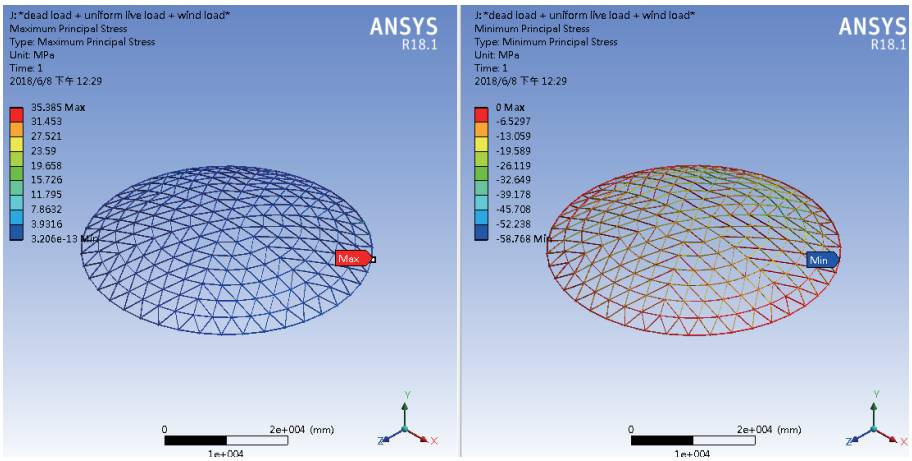

Fig. 9. (Color online) Dome 1 with static load + average live load + wind load. (a) Maximum and (b) minimum principal stresses, and (c) maximum deformation.

the static and average live loads (particularly the average live load) were applied. Consequently, the stresses induced by the average live and wind loads partially offset each other, reducing the response of the designed domes to the average live load. Therefore, the σ_1, σ_3, and maximum deformation become smaller.

3.6 Static load + uneven live load + wind load

When the static, uneven live, and wind loads were applied simultaneously, the analysis results of dome 1 (not shown here) show that σ_1 was 73.93 MPa, σ_3 was −54.88 MPa, and the maximum deformation was 30.41 mm. The analysis results of dome 2 (Fig. 10) show that σ_1 was 73.14 MPa, σ_3 was −68.21 MPa, and the maximum deformation was 55.97 mm. Apparently, as the static, uneven live, and wind loads are simultaneously applied to the designed domes 1 and 2, their σ_1, σ_3, and maximum deformation values have no apparent differences from those when only the

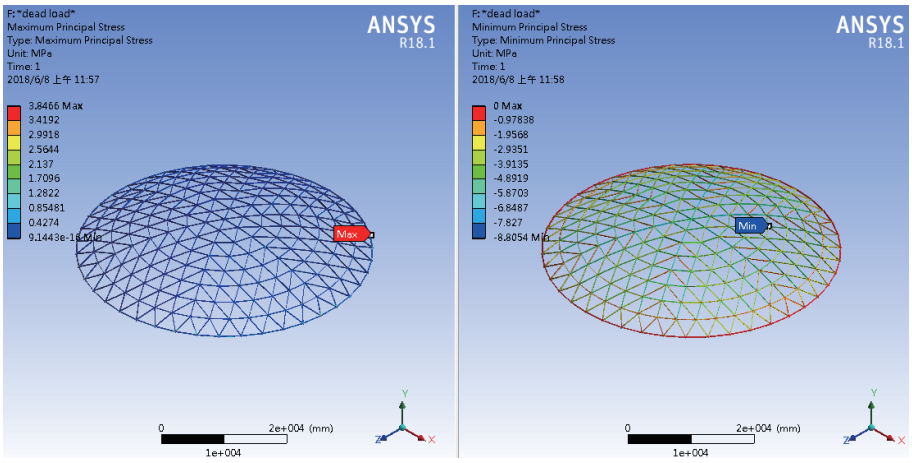

(a) (b)

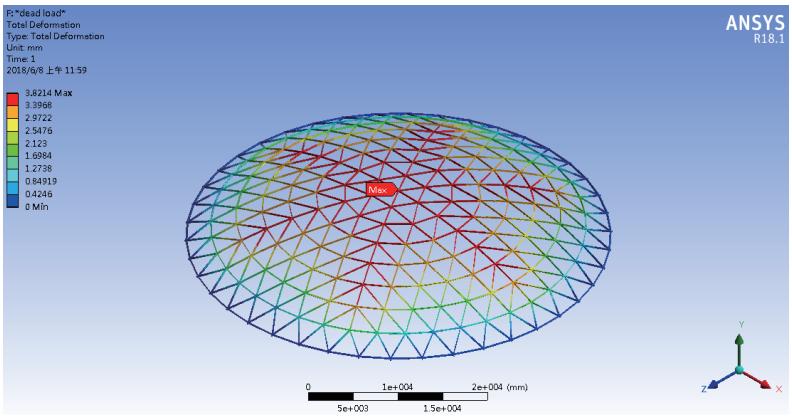

(c)

Fig. 10. (Color online) Dome 2 with static load + uneven live load + wind load. (a) Maximum and (b) minimum principal stresses, and (c) maximum deformation.

static and uneven live loads are applied simultaneously. These results prove again that the static, uneven live, and wind loads are not the most important factors that affect the safety of the designed domes, and the average live load is the most important factor.

From the simulation results, we find that none of the single-layer mesh aluminum domes designed in this study exhibit permanent deformation, and the above results demonstrate that the designed mesh aluminum domes are in compliance with safety regulations. The designed domes can evenly distribute the loads to reduce the concentrated forces applied in all the nodes. This means that the different loads are uniformly distributed in all the nodes and tubes according to the load distribution regions. Tables 4 and 5 integrate all the data to find the maximum principal stresses and deformations under different load conditions. These results show that under most load conditions, the maximum principal stress of dome 1 is smaller than that of dome 2, and all the maximum deformation values of dome 1 are much smaller than those of dome 2. Tables 4 and 5 also show that the static load + average live load condition causes dome 2 to have the maximum stress and deformation, and thus special attention must be paid to that condition when a dome is designed. However, when the six different loads are applied to the two domes, their maximum stresses are much smaller than that of the material used (6061-T6 aluminum alloy). Therefore, even the maximum deformation of 111.88 mm, which is caused by the static load + average live load, will not cause permanent deformation.

Table 4
Maximum principal stress of the designed domes as a function of different load conditions.

Load conditions	Maximum principal stress σ_{max} (MPa)	
	Dome 1	Dome 2
Static load	8.81	16.85
Static load + average live load	74.29	135.38
Static load + uneven live load	76.28	78.43
Static load + wind load	47.56	75.93
Static load + average live load + wind load	58.77	77.83
Static load + uneven live load + wind load	73.93	73.14

Table 5
Maximum deformation of the designed domes as a function of different load conditions.

Load conditions	Maximum deformation (mm)	
	Dome 1	Dome 2
Static load	3.82	13.34
Static load + average live load	32.45	111.88
Static load + uneven live load	29.62	59.21
Static load + wind load	20.37	61.67
Static load + average live load + wind load	25.35	60.11
Static load + uneven live load + wind load	30.41	55.97

4. Conclusions

In this study, the simulation results showed that as the static and uneven live loads were simultaneously applied to the domes, domes 1 and 2 had the maximum principal stress and deformation. These results prove that the static, uneven live, and wind loads are not the most important factors that affect the safety of the designed domes, and the average live load is the most important factor. Under most load conditions, the absolute value of σ_1 is less than that of σ_3, and all the maximum deformation values of dome 1 were smaller than those of dome 2. The simulation results prove that the dome with welded connections (dome 1) is stabler than that with sliding connections (dome 2). The simulation results also showed that the static load + average live load condition caused dome 2 to have the maximum stress of 135.38 MPa and the maximum deformation of 111.88 mm. The dome designed using the sliding base as its welding method will have poor security features. Thus, the safety issues of this type of dome require special attention.

Acknowledgments

This work was supported by projects under Nos. MOST 109-2221-E-390-023, MOST 110-2622-E-390-002, and MOST 110-2221-E-390-020.

References

1 Y. Uematsu, M. Yamada, A. Inoue, and T. Hongo: J. Wind. Eng. Ind. Aerodyn. **66** (1997) 227.
2 C. Wang and S. Shen: Proc. 2nd Int. Conf. Advances in Steel Structures 15–17 December 1999, Hong Kong, China (ICASS'99) (1999) 201–208.
3 Y. Uematsu, O. Kuribara, M. Yamada, A. Sasaki, and T. Hongo: J. Wind. Eng. Ind. Aerodyn. **89** (2001) 1671.
4 A. López, I. Puente, and M. A. Serna: Eng. Struct. **29** (2007) 101.
5 F. Fan, J. Yan, and Z. Cao: Thin-Walled Struct. **60** (2012) 239.
6 F. Fan, J. Yan, and Z. Cao: J. Constr. Steel Res. **77** (2012) 32.
7 H. Liu, W. Zhang, and H. Yuan: Eng. Struct. **124** (2016) 473.
8 Y. Jihong and Q. Nian: J. Constr. Steel Res. **128** (2017) 721.
9 G. B. Nie, X. D. Zhi, F. Fan, and J. W. Dai: J. Constr. Steel Res. **100** (2014) 176.
10 C. A. Dimopoulos and C. J. Gantes: Thin-Walled Struct. **96** (2015) 11.
11 A. Sharbaf, M. Bemanian, K. Daneshjoo, and H. Shakib: Buildings **11** (2021) 241.
12 D. Opatowicz, U. Rado´n, and P. Zabojszcza: Buildings **10** (2021) 179.
13 G. Nie and K. Liu: Shock Vib. **2018** (2018) 6041878.
14 C. Zhao, J. Ma, S. Du, Y. Gu, and Y. Zhou: Mater. Technol. **53** (2019) 811.
15 Z. S. Makowski: Analysis, Design and Construction of Braced Domes (Nichols Publishing, New York, 1984).
16 ANSYS 15.0. Mechanical User's Guide: Material Models Used in Explicit Dynamics Analysis (2013).